Kuwajima, K., Hiraoka, Y., Ikeguchi, M., & Sugai, S. (1985) *Biochemistry 24*, 874-881.
Lesk, A. M., & Rose, G. D. (1981) *Proc. Natl. Acad. Sci. U.S.A. 78*, 4304-4308.
Lim, V. I. (1978) *FEBS Lett. 89*, 10-14.
Lynn, R. M., Konishi, Y., & Scheraga, H. A. (1984) *Biochemistry 23*, 2470-2477.
McCoy, L. F., Jr., Rowe, E. S., & Wong, K. P. (1980) *Biochemistry 19*, 4738-4743.
Mitchinson, C., & Pain, R. H. (1985) *J. Mol. Biol. 184*, 331-342.
Mulqueen, P. M., & Kronman, M. J. (1982) *Arch. Biochem. Biophys. 215*, 28-39.
Nozaka, M., Kuwajima, K., Nitta, K., & Sugai, S. (1978) *Biochemistry 17*, 3753-3758.
Poland, D., & Scheraga, H. A. (1970) *Theory of Helix-Coil Transitions in Biopolymers*, Academic, New York and London.
Ptitsyn, O. B., & Finkelstein, A. V. (1980) *Q. Rev. Biophys. 13*, 339-386.
Robson, B., & Pain, R. H. (1976) *Biochem. J. 155*, 331-344.
Segawa, T., & Sugai, S. (1983) *J. Biochem. (Tokyo) 93*, 1321-1328.
Shewale, J. G., Sinha, S. K., & Brew, K. (1984) *J. Biol. Chem. 259*, 4947-4956.
Sugai, S., Yashiro, H., & Nitta, K. (1973) *Biochim. Biophys. Acta 328*, 35-41.
Tanaka, S., & Scheraga, H. A. (1977) *Macromolecules 10*, 291-304.
Tanford, C., Aune, K. C., & Ikai, A. (1973) *J. Mol. Biol. 73*, 185-197.
Tonomura, B., Nakatani, H., Ohnishi, M., Yamaguchi-Ito, J., & Hiromi, K. (1978) *Anal. Biochem. 84*, 370-383.
White, F. H., Jr. (1982) *Biochemistry 21*, 967-977.
Wong, K. P., & Tanford, C. (1973) *J. Biol. Chem. 248*, 8518-8523.

# Molecular Order, Dynamics, and Ionization State of Phosphatidylethanolamine Bilayers As Studied by $^{15}N$ NMR†

Serge Akoka, Charles Tellier,* and Serge Poignant
*Laboratoire de RMN et Réactivité Chimique, UA CNRS No. 472, Centre de Recherche en Biologie et Physico-Chimie Cellulaire, 44072 Nantes, France*

*Received March 21, 1986; Revised Manuscript Received July 24, 1986*

ABSTRACT: Dipalmitoylphosphatidylethanolamine (DPPE) and dipalmitoylphosphatidylcholine (DPPC), $^{15}N$-labeled in the polar head group, were synthesized. The proton-decoupled $^{15}N$ spectra of DPPC and DPPE in aqueous dispersion have exactly the form anticipated for powder line shapes governed by an axially symmetric shielding tensor. The chemical shift anisotropy ($\Delta\sigma$) of DPPC is lower than 0.4 ppm at 30 °C and vanished when the temperature or the half-height line width is increased; DPPE always exhibits an asymmetric line shape, and $^{15}N$ NMR spectra of DPPE are obtained at various temperatures and simulated to measure exactly the chemical shift anisotropy. At each temperature, the order parameter of the C-N bond segment is derivated from $\Delta\sigma$ and reveals that the average orientation of the C-N bond around the axis of rotation is near the "magic angle" (54.7°). Isotropic correlation times are derived from $T_1$, which are higher than values obtained for phosphatidylcholine by other nuclei. Arrhenius plots of $T_1$ and $T_2$ allowed us to calculate the activation energy for the motion of the DPPE and the DPPC C-N bond. The value of this activation energy for the DPPE (53 kJ/mol) is higher than the one found for the DPPC C-N bond (32 kJ/mol). These differences agree with the capacity of the ethanolamine head groups to bind noncovalently to their neighbors in the plane of the membrane surface. A direct titration curve of the amino group is achieved by the variation of the chemical shift with the bulk pH, and the interfacial $pK_a$ is calculated to be 11.1. At pH 11, two distinct protonation states of DPPE are observed, which are in slow exchange compared to the NMR time scale. The present results clearly show the great discriminating power of $^{15}N$ spectroscopy in terms of environmental changes around the nitrogen atom at the interfacial region of membranes.

Phospholipid bilayers are an integral part of biological membranes. Knowledge of the molecular structure and dynamics of phospholipids is therefore essential for an understanding of their functional role in biological membranes. Of the many techniques being used to probe the molecular environment within membranes, nuclear magnetic resonance (NMR)[1] has proved to be one of most useful methods for investigating the dynamical state of the membrane [for reviews, see Seelig and Seelig (1980) and Jacobs and Oldfield (1981)].

At the hydrophilic part of the membrane, polar head groups play an important role in ions, drug binding, and ionization properties of lipid bilayers (Siminovitch et al., 1984). It is also known that modification of the polar head group cause changes in the cooperative properties of membranes. For example, the gel to liquid-crystal phase transition occurs at a significantly higher temperature for DPPE than for DPPC (Ladbrooke & Chapman, 1969). In order to understand the influence the

† This work was supported by a research fellowship from Ministère de la Recherche et de la Technologie (to S.A.).
* Author to whom correspondence should be addressed.

[1] Abbreviations: NMR, nuclear magnetic resonance; DPPC, dipalmitoylphosphatidylcholine; DPPE, dipalmitoylphosphatidylethanolamine; EDTA, ethylenediaminetetraacetic acid; NOE, nuclear Overhauser effect.

0006-2960/86/0425-6972$01.50/0 

head group has on the properties of the lipid bilayer, a knowledge of the orientation and flexibility of the polar group is essential. Many NMR studies by $^{1}$H, $^{2}$H, $^{13}$C, $^{31}$P, and $^{14}$N have been reported in this field [see, e.g., Hauser et al. (1980), Gally et al. (1975), Brainard and Cordes (1981), and Rothgeb and Oldfield (1981)]. Consequently, all segments of the head group can be probed in a nonperturbing way.

Recently, we have used $^{15}$N NMR spectroscopy in a study of a model membrane system consisting of an aqueous dispersion of $^{15}$N-enriched DPPC (Tellier et al., 1985). Despite the necessity of isotopic labeling, the $^{15}$N NMR technique is shown to be useful in determining the dynamic structure of the choline head group. Furthermore, it is the only way of studying amine-containing head groups at the nitrogen level because the nitrogen-14 quadrupole tensor is too large to obtain detectable $^{14}$N NMR lines with non-choline head groups like phosphatidylethanolamine (Edmonds & Summers, 1973).

In this paper, we show the potentialities of $^{15}$N NMR for investigating the dynamics and the conformation of the phosphatidylethanolamine head groups. Anisotropic lines are obtained from $^{15}$N-enriched DPPE, which are interpreted in terms of the order parameter of the C–N bond. The reorientational correlation time of the N–$CH_2$ axis is deduced from measurements of the $T_1$ relaxation time, and ionization properties of the amine group are studied from the pH dependence of the chemical shift.

## Materials and Methods

*Synthesis of $^{15}$N-Enriched Phospholipids.* Nitrogen-15-labeled DPPC and DPPE were synthesized by transphosphatidylation of commercial DPPC (Sigma) with phospholipase D according to published procedures (Akoka et al., 1985). Phospholipase D was extracted from Brussels sprouts (Davidson & Long, 1958). Amino alcohols, [$^{15}$N]glycine, and [$^{15}$N]choline were purchased from CEA France. [$^{15}$N]-Ethanolamine was prepared by esterification of [$^{15}$N]glycine and reduction of the glycine methyl ester after tritylation of the amine function. This protecting group was removed after the reduction by the action of acetic acid. Labeled phospholipids were purified by high-performance liquid chromatography (Waters) on a $\mu$-Porasil column (10 $\mu$m) with $CHCl_3$–$CH_3OH$–$NH_4OH$–$H_2O$ (68:28:2:2) as solvent.

The amount of purified phospholipids was determined by phosphorus analysis (Rouser et al., 1970). The $^{15}$N enrichment of DPPC was measured by infrared FT (Bruker I.F.S. 45), the DPPC $^{14}$N band at 871.5 cm$^{-1}$ being shifted to 863.5 cm$^{-1}$ for DPPC $^{15}$N.

*Sample Preparations.* Multilayered liposomes of phospholipids were prepared by vortexing a weighed amount of phospholipid above their gel to liquid-crystal phase transition temperature in 2 mL of citrate buffer, pH 7, containing 2 mM EDTA. Samples transferred in a 10-mm NMR tube were stabilized by several cycles of freezing and thawing.

For DPPE, the pH was varied from 7 to 11 by adding buffering solution made of carbonate, 80 mM, and NaOH, 1 M. These pH adjustments were performed above the phase-transition temperature, and the pH was measured at 20 °C after several freeze–thaw cycles for stabilization. pH was found unchanged after NMR experiments.

*NMR Measurements.* $^{15}$N NMR spectra were obtained at 25.398 MHz on a Bruker WM 250 spectrometer, interfaced with an Aspect 2000 computer. Typically, 8000 scans were acquired in the quadrature mode by using a spectral width of 10 kHz and a pulse angle of 40° (50-$\mu$s duration). This phase of the pulse was cycled ($x$, $y$, $-x$, $-y$) to minimize spectral images due to missettings of the relative gain and phase pulse of the quadrature phase sensitive detectors (Stejskal & Schaefer, 1974). All spectra were obtained in the presence of maximum power broad-band proton decoupling (15 W) during the acquisition time (102.4 ms corresponding to 2048 time domain data points) and a reduced power (3 W) during the relaxation delay (0.7 s) in order to limit heating effects. The spin–lattice relaxation time $T_1$ was measured by the inversion–recovery method and calculated by fitting the experimental points to a three-parameter equation. NOE measurements were made with an appropriate pulse sequence (Granger et al., 1980) to limit heating effects and to avoid a drift in field homogeneity.

Spectral simulations were carried out on an IBM A.1130 computer using a FORTRAN program that performs a line-shape calculation of powder-type spectra according to the equation proposed by Seelig (1978).

## Theory

The observed $^{15}$N NMR spectrum of the $^{15}$N-labeled DPPE liposomes clearly shows an anisotropic feature (Figure 1) that can be readily described as a powder-pattern line shape arising from the anisotropic $^{15}$N chemical shift. In phospholipid membranes, the interpretation of the observed chemical shift anisotropy in terms of molecular order has been previously described for the phosphorus nucleus (Seelig, 1978; Campbell et al., 1979), the carbon-13 nucleus (Cornell, 1981), and the fluorine nucleus (Gent & Ho, 1978). Here, we briefly present how the $^{15}$N chemical shift anisotropy can be related to the order parameter of the C–N bond.

In presence of a high-power broad-band decoupling to eliminate heteronuclear dipolar interactions between the nitrogen and its nearby protons, the interaction of the nucleus with the static magnetic field can be described by

$$H_z = -\vec{\mu}(1 - \sigma)\vec{H}_0$$

where $\sigma$ is the chemical shift anisotropy tensor:

$$\sigma = \begin{Vmatrix} \sigma_{11} & 0 & 0 \\ 0 & \sigma_{22} & 0 \\ 0 & 0 & \sigma_{33} \end{Vmatrix}$$

The bilayer structure is characterized by a rapid rotation of the lipid molecules around the bilayer normal. Due to this motion, the static chemical shielding is averaged to a new effective axially symmetric tensor:

$$\bar{\sigma} = \begin{Vmatrix} \sigma_\perp & 0 & 0 \\ 0 & \sigma_\perp & 0 \\ 0 & 0 & \sigma_\parallel \end{Vmatrix}$$

The time-averaged tensor elements $\sigma_\parallel$ and $\sigma_\perp$ are related to the element of the static tensor $\sigma$ so that the shielding anisotropy in liquid crystalline bilayers is given by

$$\overline{\Delta\sigma} = \sigma_\parallel - \sigma_\perp = S_{11}(\sigma_{11} - \sigma_{22}) + S_{33}(\sigma_{33} - \sigma_{22})$$

$S_{ii}$ are the so-called order parameters:

$$S_{ii} = \tfrac{1}{2}\overline{(3\cos^2\theta_i - 1)}$$

where $\cos\theta_i$ ($i$ = 1, 2, 3) are the direction cosines between the axis of rotation and the principal axes of the shielding tensor.

In DPPE and DPPC, the major contribution to the chemical shielding comes respectively from the electronic environment of the $CH_2$–$NH_3$ and the $CH_2$–$N(CH_3)_3$ groups. Since these groups possess a $C_{3v}$ symmetry axis, we can safely assume that the shielding tensor is axially symmetric ($\sigma_{11} = \sigma_{22}$) and that the principal symmetry axis of the tensor coincides with the C–N bond. The chemical shift anisotropy becomes

$$\overline{\Delta\sigma} = S_{C\text{-}N}(\sigma_{33} - \sigma_{22}) \quad (1)$$

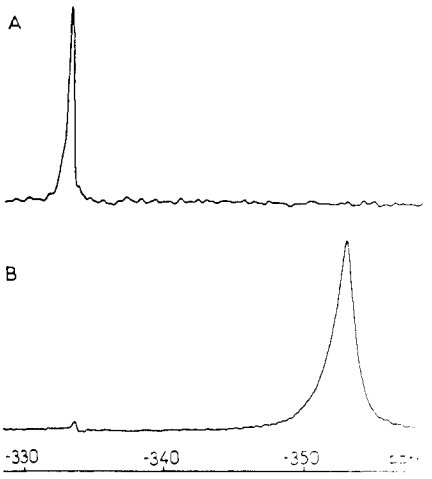


FIGURE 1: The 25.35-MHz $^{15}N$ NMR spectra of unsonicated dispersions of (A) DPPC and (B) DPPE. Both spectra were recorded at 30 °C; 16 000 free induction decays were averaged. The DPPC spectrum has a 1-Hz line broadening due to exponential multiplication. The chemical shifts were measured with an external reference of enriched nitromethane: 0.005 $cm^3$ of $CH_3NO_2$–0.35 $cm^3$ of $CD_3NO_2$–2 mg of $Cr(acac)_3$. For DPPC $\delta = -333.7$ ppm, and for DPPE $\delta = -352.7$ ppm.

where $S_{C-N}$ is the order parameter of the C–N bond.

Then, the knowledge of $\overline{\Delta\sigma}$ and $\sigma_{33} - \sigma_{22}$ allows the calculation of the average conformation of the amino group within the bilayer.

Unfortunately, up till now, few data on $^{15}N$ chemical shift tensors have been published presumably because of the difficulty of detecting nuclear signals for this low-abundance, low gyromagnetic ratio spin. However, a small shift anisotropy of the $NH_3$ group (~10 ppm) has been observed in solid glycine, lysine, asparagine, and the glycylglycine peptide (Harbison et al., 1981).

## RESULTS

The chemical shift difference between $^{15}N$-labeled DPPC and DPPE in aqueous dispersion is illustrated in Figure 1. It is to be noted that the difference ($\Delta\delta = 19.7$ ppm) is larger than the spectral width of each line, allowing an easy investigation of each component in a phospholipid mixture to be performed. At 30 °C, DPPC is below the phase transition temperature and exhibits a highly symmetrical line shape where the chemical shift anisotropy $\Delta\sigma$, estimated from a computer simulation, is lower than 0.4 ppm. This anisotropy becomes not detectable when the width at half-height increases by lowering of the temperature or by insufficient proton-decoupling power.

Figure 2A shows $^{15}N$ NMR spectra of aqueous dispersions of labeled DPPE for different temperatures above and below the gel to liquid-crystal phase transition. Clearly, these lines are characterized by an anisotropic feature resulting from the superposition of spectra of randomly oriented C–N bonds. The $^{15}N$ chemical shift anisotropy $\Delta\sigma$, which corresponds to the separation of the edges in the powder-type spectra, cannot be easily measured on these spectra. A more accurate value is obtained by a computer simulation (Seelig, 1978) of the spectra, and the theoretical spectra (Figure 2B) are obtained on the basis of the best fit from all the relevant parameters: the $^{15}N$ chemical shift anisotropy ($\Delta\sigma$), the isotropic line width at half-height ($\Delta\nu_{iso}$), and the anisotropic line width ($\Delta\nu_{aniso}$) taking into account line broadening by residual dipolar couplings and anisotropic relaxation. The values determined for $\Delta\sigma$ are plotted as a function of the temperature in Figure 3. The decrease of $\Delta\sigma$ with increasing temperature is consistent

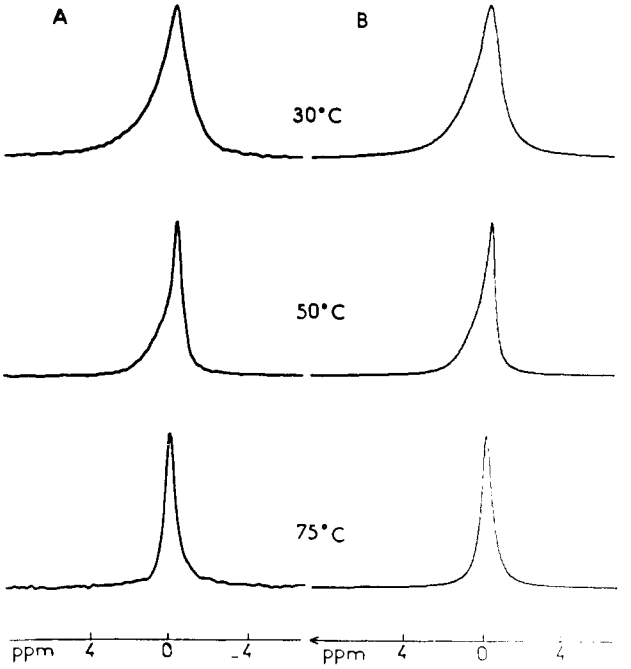


FIGURE 2: The 25.35-MHz $^{15}N$ NMR spectra of unsonicated aqueous dispersions of DPPE: (A) FT spectra and (B) simulations. A total of 8K scans was averaged, except for the 30 °C spectrum where 16K were used. All spectra were recorded at pH 6.8. The zero reference is arbitrarily put on the chemical shift of DPPE at 30 °C and pH 6.8.

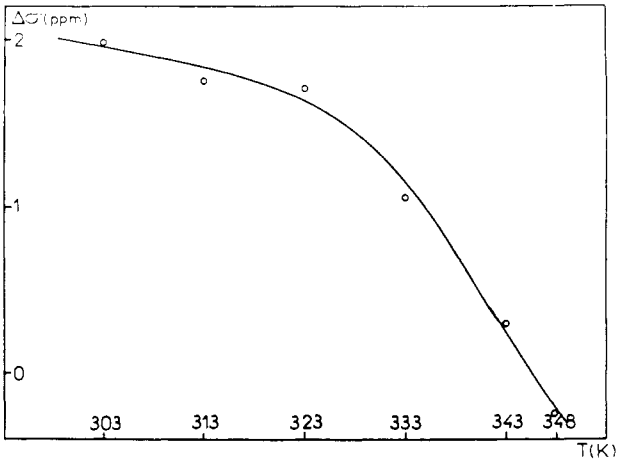


FIGURE 3: Temperature dependence of the nitrogen-15 chemical shift anisotropy (in ppm) for DPPE in unsonicated aqueous dispersions.

with less order and greater mobility of the C–N bond. Maximum variation is obtained around the gel to liquid-crystal transition temperature (63 °C), showing that hydrocarbon melting affects the order of the polar head group. It should be noted that the absolute value of the $^{15}N$ shielding anisotropy is small and that its sign changes during the phase transition (cf. Figure 3). This fact demonstrates that the average orientation and angular fluctuations of the C–N bond around the axis of rotation are near the so-called "magic angle" (54.7°).

The transverse relaxation time $T_2$ was estimated from the line width at half-height ($\Delta\nu_{iso}$) determined by computer simulations of the spectra [$T_2 = (\pi\Delta\nu_{iso})^{-1}$]. $T_2$ decreases from 430 ms at 75 °C to 40 ms at 30 °C. The $^{15}N$ spin–lattice relaxation time ($T_1$) determined by an inversion–recovery pulse sequence (Freeman & Hill, 1971) varies from 4.7 s at 60 °C to 300 ms at 30 °C for the DPPE and from 57.1 s at 60 °C to 22.3 s at 35 °C for the DPPC. As observed in studies

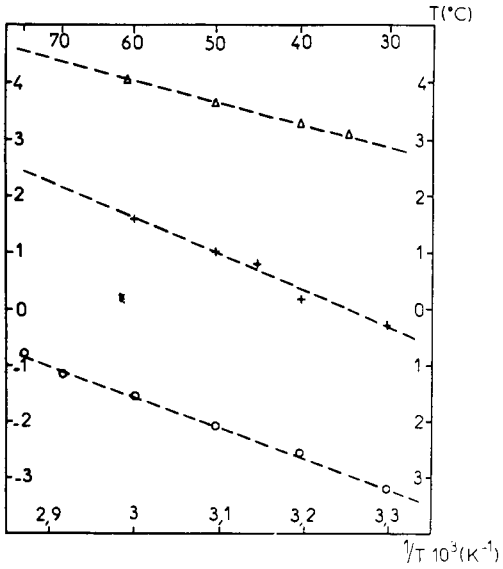


FIGURE 4: Arrhenius plot of $^{15}$N spin–lattice relaxation times, $T_1$ [DPPE (+), DPPC (Δ)], and spin–spin relaxation times, $T_2$ [DPPE (O)]. $T_1$ values were obtained by the inversion–recovery method while $T_2$ values were calculated from the half full width $\Delta\nu_{iso}$ obtained by computer simulation.

employing other nuclei, the $^{15}$N $T_2$ value was always 10–20 times shorter than the $^{15}$N $T_1$ in membrane systems, according to the low-frequency molecular dependence to $T_2$ (Koga & Kanazawa, 1980). The $T_1$ relaxation time decreases with decreasing temperature, indicating that relaxation time was in the short correlation time regime ($\omega_0\tau_c < 1$, $\omega_0 = 2.5 \times 10^8$ rad·s$^{-1}$, where $\omega_0$ is the NMR resonance frequency for nitrogen and $\tau_c$ is the molecular correlation time of the amino group). Arrhenius plots for the $T_1$ and $T_2$ data are given in Figure 4. A linear relation is obtained in both cases despite the presence of a temperature transition at 41 °C for DPPC and 63 °C for DPPE, and from the slope, we calculated the apparent activation energies for the motions involved in $T_1$ (53 kJ/mol for the DPPE, 32 kJ/mol for the DPPC) and $T_2$ (44 kJ/mol for the DPPE). The DPPE value appears slightly greater than those derived from $^2$H $T_1$ studies for the $C_\alpha$ and $C_\beta$ segment position (Browning, 1981) while the DPPC result is consistent with one found by $^{14}$N NMR (Siminovitch et al., 1984).

In order to determine the mechanism that is responsible for the relaxation rate, we measured the nuclear Overhauser effect (NOE) at 30 °C. The value of $\eta$ [$\eta = (I - I_0/I_0 = -4.4$] found is very close to the theoretical maximum, −4.93, so we can say that the relaxation time $T_1$ is mainly goverened by a purely dipolar mechanism. Similar results have been obtained for aqueous $^{15}$N DPPC (Tellier et al., 1985).

$^{15}$N chemical shifts of amine groups are very sensitive to the state of ionization of these groups ($\Delta\delta$ = 13 ppm). Assuming that the dissociation $NH_3^+ \rightleftarrows NH_2 + H^+$ is fast over the NMR time scale at room temperature, a titration curve of amine group can be achieved by measuring the variation of $^{15}$N chemical shift with the bulk pH. Figure 5 shows the NMR titration curve for ethanolamine in water and DPPE in bilayers. The apparent p$K_a$ for aqueous ethanolamine is thus defined by the bulk pH value corresponding to half-dissociation (p$K_a \simeq 9.1$). For DPPE, the dissociation coefficient defined as

$$\alpha = \frac{[NH_2]}{[NH_2] + [NH_3^+]} = \frac{\Delta\delta_{measd}}{\Delta\delta_{max}}$$

is only 45% at pH 11, and the p$K_a$ can be calculated to approximatively 11.1, which is more than 2 units higher than

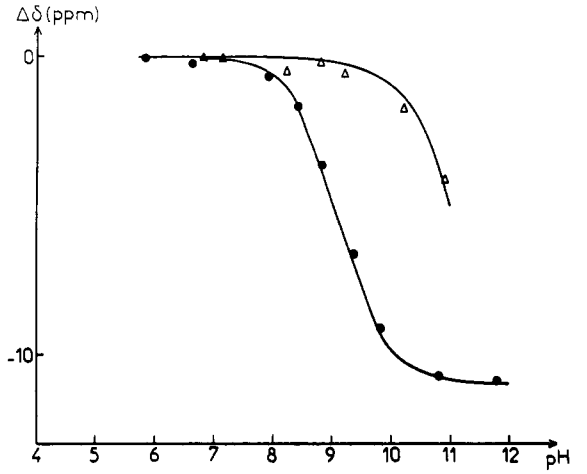


FIGURE 5: NMR titration of amino group for ethanolamine in solution (●) and for DPPE in aqueous dispersions (Δ). $T$ = 300K, 20 mM citrate buffer, and addition of 0.8 M carbonate buffer for pH 9. Curves are fitted to the Henderson–Hasselbach equation.

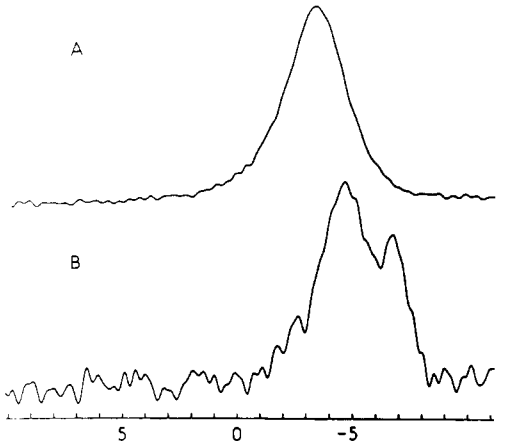


FIGURE 6: The 25.35-MHz $^{15}$N NMR spectra of DPPE in aqueous dispersions at pH 10 (A) and pH 11 (B). $T$ = 300K and carbonate–bicarbonate buffer. A total of 8K scans was averaged for both spectra.

the normal p$K_a$. These results are in agreement with a previous phosphatidylethanolamine titration curve obtained by differential scanning calorimetry (Traüble & Eibl, 1974).

Figure 6 shows the spectra of $^{15}$N DPPE at 30 °C for two different pH values. Compared to the spectra obtained at low pH (Figure 2), these spectra are characterized by a higher line width, which is in apparent contradiction with the lowering of the phase transition temperature of DPPE at high pH (Seelig & Gally, 1976). Furthermore at pH 11, the line shape reflects the presence of at least two distinct species. By lowering the pH, we observe that these changes are fully reversible, demonstrating that the two species do not correspond to a chemical degradation of DPPE. After this treatment, DPPE give a single spot in thin-layer chromatography.

## Discussion

Extensive neutron diffraction studies on the phosphatidylethanolamine head group orientation in single crystals (Hitchcock et al., 1974) or in the liquid-crystalline state (Büldt & Seelig, 1980) have demonstrated that the average orientation of the phosphoethanolamine dipole is nearly parallel to the membrane surface. $^2$H and $^{31}$P NMR head group studies have confirmed this boomerang-shaped conformation where the bilayer normal acts as an axis of symmetry (Seelig & Seelig, 1980; Seelig & Gally, 1976).

We have found that [$^{15}$N]DPPE line shapes are modulated by a chemical shift anisotropy ($\Delta\sigma$) that can be related to the

order parameter of the C–N bond (see Theory). This interpretation of the $^{15}N$ $\Delta\sigma$ is valuable as long as the static anisotropy ($\sigma_{33} - \sigma_{22}$) remains constant. For example, deprotonation of the amine group at high pH leads to a loss of the $C_{3v}$ symmetry of the C–N bond, leading to a modification of the static chemical shift anisotropy. Changes in $\Delta\sigma$ can no longer be analyzed in terms of $S_{C-N}$ variation. However at pH 8, the DPPE amine group is fully protonated (see Figure 5), and we used the static chemical shift anisotropy value at ~10 ppm observed for various amines (Harbison et al., 1981) to calculate $S_{C-N}$. From eq 1 (Theory), it was deduced that the values of $S_{C-N}$ for DPPE are nearly identical with those observed for DPPC from $^{14}N$ quadrupole splitting measurements (Siminovitch et al., 1980). Because the value of $S_{C-N}$ will, in general, depend on both (i) the average orientation of the C–N bond segment with respect to the axis of rotational symmetry (the bilayer normal) and (ii) the amplitude of fluctuations around this average orientation it is not possible to unequivocally attribute the observed decrease in $S_{C-N}$ with temperature to a change in the average orientation of the C–N bond segment. However, comparison between the temperature profiles of $\Delta\sigma$ (Figure 3) and the relaxation times (Figure 4) reveals the absence of a jump in the relaxation time. The Arrhenius plots around the transition temperature suggest that the amplitude of the C–N bond vector fluctuations about the axis of motional averaging does not suddenly change through the phase transition. Thus, only the average orientation of the C–N bond could be responsible for the $S_{C-N}$ variation with temperature. Furthermore, the sign inversion of the anisotropy between 70 and 75 °C (Figure 3) indicates that the angle between the orientation of the C–N bond and the normal bilayer is around 55 °C (the so-called magic angle that satisfies the equation $3\cos^2\theta - 1 = 0$). This value is consistent with the conformation obtained by $^{31}P$ and $^{2}H$ (Seelig & Gally, 1976) for the polar head group of DPPE in aqueous dispersion allowing the layer-parallel orientation of the P–N dipole.

Dynamic information on the rate of molecular motion can be provided by $^{15}N$ relaxation time measurements. It has been suggested that the spin–lattice relaxation times of $^{2}H$, $^{13}C$ (Brown et al., 1983), and $^{14}N$ (Kanazawa et al., 1985) in lipid bilayers depend on both (i) rapid, local motions with a correlation time $\tau_c$ less than $1/\omega_0$ (where $\omega_0$ is the NMR resonance frequency) and (ii) collective bilayer fluctuations producing a frequency dependence of $T_1$. For these nuclei, $T_1$ can be described by a relaxation law of the form $T^{-1} = A\tau_c + BS^2\omega^{1/2}$. In our case, the $^{15}N$ $T_1$ rate will be expressed in terms of the reorientational correlation time and order parameter of the C–N bond. According to the low value of $S_{C-N}$ in DPPE, we can neglect the frequency-dependent term in the relaxation law. The high negative value of the $^{15}N$ NOE measured in DPPE and DPPC demonstrated that the dominant relaxation mechanism is dipolar. Furthermore, the increase in $T_1$ with temperature demonstrated that local segmental motions ($\tau_c$ of the C–N bond satisfied the extreme narrowing condition) $\tau_c\omega_0 \ll 1$ at 25.4 MHz. Thus, the $^{15}N$ spin–lattice relaxation time of DPPE can be approximated by the following relation (Abragam, 1961):

$$1/T_1 = \frac{\mu_0^2}{16\pi^2}[n/(4\pi^2)](\gamma_H^2\gamma_N^2h^2/r^6)\tau_c$$

where $n$ is the number of $^{1}H$ nuclei that are dipolar-coupled to $^{15}N$ at a distance of $r$ and $\gamma$'s are the magnetogyric ratios of the respective nuclei. The correlation time for the fast reorientation about the C–N axis is on the order of $2.3 \times 10^{-10}$ to $1.5 \times 10^{-10}$ s for the DPPE and $1 \times 10^{-10}$ to $0.5 \times 10^{-10}$ s for the DPPC in the temperature ranges. It must be noted that these values explain the result of the NOE experiments since the maximum enhancement at 25.35 MHz was 4.6 for $\tau \simeq 2 \times 10^{-10}$ s (Martin et al., 1981).

The activation energies for the motion of the DPPE C–N bond deduced from $T_1$ measurements (53 kJ/mol) and $T_2$ measurements (44 kJ/mol) are higher than that found for the DPPC C–N bond (32 kJ/mol), presumably reflecting a higher energy barrier to rotation of the amine head group. Similar results have been obtained with $^{2}H$ NMR (Browning, 1981), which would be explained by the existence of a proton-transfer complex between the amine and phosphate group of two vicinal lipid molecules (Hauser & Phillips, 1979). Phosphatidylcholine cannot form a proton-transfer complex and can only interact electrostatically. Extensive interactions within the plane of the membrane are favored by the head group conformation parallel to this plane (Büldt & Seelig, 1980). These noncovalent interactions appear to render the phosphatidylethanolamine head group less flexible as it has been shown by the low changes in the order parameter of the C–N bond.

This proton-transfer complex for the phosphatidylethanolamine head group could also be responsible for the shift in the $pK_a$ of the amine group observed by NMR titration (Figure 5). Thus, the molecular interactions due to this complex modify the interfacial acid–base equilibrium of the amine group as has been already shown for fatty amines incorporated in phosphatidylcholine vesicles (Ptak et al., 1980).

The changes observed in the $^{15}N$ line shape with increasing pH (Figure 6) cannot be interpreted directly by a modification of the C–N bond order parameter since the static chemical shift anisotropy increases in the deprotonated amine. For example, the chemical shift anisotropy is respectively equal to about 10 ppm (Gibby et al., 1972) and 100 ppm (Munowitz et al., 1984) for the $NH_3$ and $NH_2$ groups in glycine and asparagine. Because the static anisotropy of deprotonated DPPE is unknown, it is not possible, at this time, to go further in the interpretation of the $^{15}N$ line shapes at high pH. However, at pH 11 we observed the presence of at least two distinct species that are in slow exchange compared to the NMR time scale (Munowitz et al., 1982). At pH 10, only one shifted line is observed, demonstrating that the ionic equilibrium is fast on the NMR time scale and the chemical shift depends on the dissociation coefficient. The two lines could arise from (i) a heterogeneous pH distribution within the lipid multilayered sample despite the stabilization procedure described under Materials and Methods or (ii) the appearance of a phase separation between protonated and nonprotonated DPPE at the surface of the membrane. Further studies of the pH dependence of the $^{15}N$ line shape are now in progress to explain these results.

## Conclusions

The results presented in this paper demonstrate that $^{15}N$ NMR is a powerful tool for the study of aqueous phospholipids dispersions, in spite of the low magnetogyric ratio of this nucleus. The line-shape analysis of the $^{15}N$-labeled phospholipid was found to be very convenient to determine the value of the order parameter of the C–N bond. The result obtained for DPPE confirms those previously proposed with other nuclei or other techniques. The spin–lattice relaxation study allowed us to compute a correlation time of on the order $2 \times 10^{-10}$ s, which is characteristic of the molecular motion of the amino group. This value is in good agreement with the results obtained by $^{14}N$ NMR for phosphatidylcholine bilayers (Kanazawa et al., 1985). The higher correlation time observed for phosphatidylethanolamine than for phosphatidylcholine

is also consistent with the value of the activation energy (50 kJ/mol) found for DPPE, which is substantially greater than the $E_a$ value of DPPC. $^{15}$N NMR allows a direct study of the primary amino group to be performed and therefore offers a great advantage over $^{14}$N NMR, which is limited to the non-protonated amino group. Moreover, isotropic chemical shifts of phosphatidylcholine and phosphatidylethanolamine differ by about 20 ppm, so this probe has another advantage over previously studied nuclei since it will allow the observation of separate signals for both components of a mixture of the two classes of phospholipids. Finally, a more striking advantage of $^{15}$N NMR spectroscopy is perhaps the great discriminating power of this isotope in terms of environmental changes around the nitrogen atom, especially with interfacial pH in phosphatidylethanolamine bilayers.

## ACKNOWLEDGMENTS

We thank Dr. D. Le Botlan for helpful assistance in computer simulations and Dr. G. J. Martin for comments and criticism during the course of this investigation.

**Registry No.** DPPE, 3026-45-7; DPPC, 2644-64-6; [$^{15}$N]DPPE, 104576-74-1; [$^{15}$N]DPPC, 98292-01-4; $^{15}$N, 14390-96-6; $H_2{}^{15}NCH_2CO_2H$, 7299-33-4; $H_2{}^{15}NCH_2CO_2Me$, 104576-76-3; $HO(CH_2)_2{}^{15}NH_2$, 33598-78-6.

## REFERENCES

Abragam, A. (1961) *The Principles of Nuclear Magnetism*, Oxford University Press, London.

Akoka, S., Meir, C., Tellier, C., Belaud, C., & Poignant, S. (1985) *Synth. Commun. 15*, 101–107.

Brainard, J. R., & Cordes, E. H. (1981) *Biochemistry 20*, 4607–4617.

Brown, M. F., Ribeiro, A. A., & Williams, G. D. (1983) *Proc. Natl. Acad. Sci. U.S.A. 80*, 4325–4329.

Browning, J. L. (1981) *Biochemistry 20*, 7144–7159.

Büldt, G., & Seelig, J. (1980) *Biochemistry 19*, 6170–6175.

Campbell, R. F., Meirovitch, E., & Freed, J. H. (1979) *J. Phys. Chem. 83*, 525–533.

Cornell, B. A. (1981) *Chem. Phys. Lipids 28*, 69–78.

Davidson, F. M., & Long, C. (1958) *Biochem. J. 69*, 458–466.

Edmons, D. T., & Summers, C. P. (1973) *J. Magn. Reson. 12*, 134–142.

Freeman, R., & Hill, H. C. W. (1971) *J. Chem. Phys. 54*, 3367–3377.

Gally, H. U., Niederberger, W., & Seelig, J. (1975) *Biochemistry 14*, 3647–3652.

Gent, M. P. N., & Ho, C. (1978) *Biochemistry 17*, 3023–3088.

Gibby, M. G., Griffin, R. G., Pines, A., & Waugh, J. S. (1972) *Chem. Phys. Lett. 17*, 80–87.

Granger, P., Chapelle, S., & Poirier, J. M. (1980) *Org. Magn. Reson. 14*, 69–73.

Harbison, G., Herzfeld, J., & Griffin, R. G. (1981) *J. Am. Chem. Soc. 103*, 4752–4754.

Hauser, H., & Phillips, M. C. (1979) *Prog. Surf. Membr. Sci. 13*, 297–413.

Hauser, H., Guyet, W., Pasher, J., Skarabal, P., & Sundell, S. (1980) *Biochemistry 19*, 366–373.

Hitchcock, P. B., Mason, R., Thomas, K. M., & Skipley, G. G. (1974) *Proc. Natl. Acad. Sci. U.S.A. 71*, 3036–3040.

Jacobs, R. E., & Oldfield, E. (1981) *Prog. Nucl. Magn. Reson. Spectrosc. 14*, 113–136.

Kanazawa, Y., Koga, K., & Nishizono, I. (1985) *J. Magn. Reson. 62*, 518–520.

Koga, K., & Kanazawa, Y. (1980) *Biochemistry 19*, 2779–2783.

Ladbrooke, B. D., & Chapman, D. (1969) *Chem. Phys. Lipids 3*, 304–367.

Martin, G. J., Martin, M. L., & Gouesnard, J. P. (1981) *$^{15}$N-N.M.R. Spectroscopy*, Springer-Verlag, Berlin, Heidelberg, and New York.

Munovitz, M. G., Bachouchin, W. W., Herzfeld, J., Dobson, C. M., & Griffin, R. (1982) *J. Am. Chem. Soc. 104*, 1192–1196.

Munovitz, M. G., Huang, T. H., Dobson, C. M., & Griffin, R. G. (1984) *J. Magn. Reson. 57*, 56–64.

Ptak, M., Egret-Charlier, M., Sanson, A., & Bouloussa, O. (1980) *Biochim. Biophys. Acta 600*, 387–397.

Rothgeb, T. M., & Oldfield, E. (1981) *J. Biol. Chem. 256*, 6004–6009.

Rouser, G., Fleisher, S., & Yamamoto, A. (1970) *Lipids 5*, 494–496.

Seelig, J. (1978) *Biochim. Biophys. Acta 515*, 105–140.

Seelig, J., & Gally, H. U. (1976) *Biochemistry 15*, 5199–5204.

Seelig, J., & Seelig, A. (1980) *Q. Rev. Biophys. 13*, 19–61.

Siminovitch, D. J., Rance, M., & Jeffrey, K. R. (1980) *FEBS Lett. 112*, 79–82.

Siminovitch, D. J., Brown, M. F., & Jeffrey, K. R. (1984) *Biochemistry 23*, 2412–2420.

Stejskal, E. O., & Schaefer, J. (1974) *J. Magn. Reson. 14*, 160–169.

Tellier, C., Malnoë, P., & Poignant, S. (1985) *Org. Magn. Reson. 22*, 727–729.

Traüble, H., & Eibl, H. (1974) *Proc. Natl. Acad. Sci. U.S.A. 71*, 214–219.